Electrohydrodynamic Turbulent Flow in a Wide Wire-Plate Electrostatic Precipitator Measured by 3D PIV Method

J. Podlinski[1*], A. Niewulis[1], J. Mizeraczyk[1,2]
(1 Centre for Plasma and Laser Engineering, The Szewalski Institute of Fluid Flow Machinery,
Polish Academy of Sciences, Fiszera 14, 80-952 Gdańsk, Poland, *E-mail: janusz@imp.gda.pl
2 Department of Marine Electronics, Gdynia Maritime University,
Morska 81-87, 81-225 Gdynia, Poland)

Abstract: In this paper, results of 3-dimensional Particle Image Velocimetry (3D PIV) measurements of the flow velocity fields in a relatively wide wire-plate type ESP are presented. The ESP used in this work was an acrylic parallelepiped (10 cm × 20 cm × 100 cm) with a wire discharge electrode and two plate collecting electrodes. Air flow seeded with a cigarette smoke was blown along the ESP duct with an average velocity of 0.6 m/s. Either positive or negative DC voltage was applied to the wire electrode through a 10 MΩ resistor. The applied voltage was up to 28 kV. The 3D PIV velocity fields measurements were carried out in four parallel planes stretched along the ESP duct, perpendicularly to the wire electrode and plate electrodes. The measured flow structures show complex nature of the EHD-induced secondary flow in the ESP. The measured flow was turbulent and exhibit 3D structures caused by the side-wall effect.

Keywords: Wire-plate ESP, Electrohydrodynamic flow, Particle Image Velocimetry

1 INTRODUCTION

Electrostatic precipitators (ESPs) have been widely used for dust particles collection since decades. Nowadays they are very efficient when the total mass of collected dust particle is considered. However, still there is a problem with the collection efficiency of most dangerous for human health submicron particles[1].

The precipitation of particles in the ESP duct depends on the dust-particle properties, electric field, electric space charge and gas flow field[2]. The primary gas flow (that entering the ESP) is disturbed by the electrohydrodynamic (EHD) secondary flow generated in the ESP. The EHD secondary flow causes considerable changes and turbulences in the primary flow structures. There are many evidences which show that the flow turbulences are responsible for the low collection efficiency of submicron particles[3,4]. Therefore, measurements of the flow structures and turbulences in ESPs are important for better understanding the collection process in ESPs, and then for better designing of ESPs to improve the collection efficiency of submicron particles.

This work was aimed at measurements of time and space-behavior of the electrohydrodynamic (EHD) turbulent secondary flow in a wide wire-plate ESP using 3-dimensional Particle Image Velocimetry (3D PIV) [5] method.

2 EXPERIMENT

The apparatus used in this experiment consisted of an ESP, DC high voltage supply and a standard 3D PIV equipment for the flow velocity field measurement (Fig. 1).

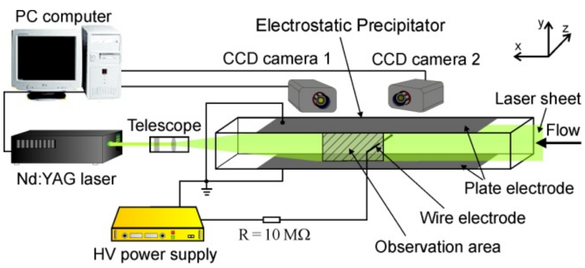

Fig. 1 Experimental set-up for 3D-PIV flow velocity field measurements in ESP

The wide-type ESP used in this work was an acrylic parallelepiped 1000 mm long, 200 mm wide and 100 mm high (width:height = 2). The electrode set consisted of a wire discharge electrode and two collecting plate electrodes. The wire electrode (diameter 1 mm, length 200 mm) was placed perpendicularly to the main flow, in the middle of the ESP between the plate electrodes, which were placed on the top and bottom of the ESP. The width of each plate electrodes was 200 mm, while the plate-to-plate electrode spacing was 100 mm. A flow homogenizer was placed before the ESP inlet.

Air flow seeded with a cigarette smoke (majority of smoke particles lower than 1m in dry air) was blown along the ESP duct with an average velocity of 0.6 m/s. Either positive or negative DC voltage of up to 28 kV was applied to the wire electrode through a 10 MΩ resistor, while the plate electrodes were grounded. The averaged discharge current was up to 130 A for positive voltage polarity and up to 150 A for negative voltage polarity.

The standard 3D PIV equipment consisted of a twin second harmonic Nd-YAG laser system (=532 nm), imaging optics (cylindrical telescope), two CCD cameras and a PC computer with Dantec FlowManager software.

The 3D PIV measurements were carried out in four parallel planes placed perpendicularly to both electrodes. The first plane (Plane A) was placed in the ESP midplane when the other (Planes B, C and D) were placed 60 mm, 20 mm and 10 mm from the side wall (Fig. 2).

The observation area (the area of the laser sheet "seen" by both CCD cameras) covered a region between the plate electrodes, ranging from 15 mm towards the flow upstream direction to 205 mm towards the flow downstream direction, when measured from the wire electrode (Fig. 1).

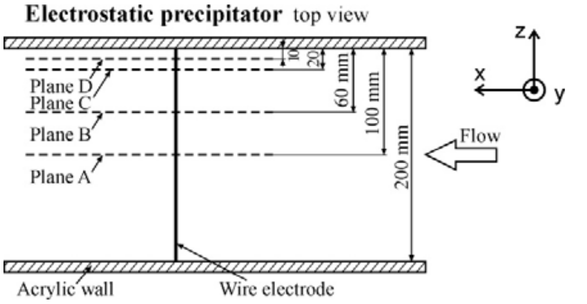

Fig. 2 ESP top view. Measurement planes A, B, C and D marked by dashed lines

3 RESULTS

Figs. 3 and 4 show the results of the PIV measurements in the ESP when no voltage was applied. The Reynolds number was Re=$V \times L/\nu$=3820[6]. The parameters used to calculate Re were: the primary flow average velocity V=0.6 m/s, the characteristic length (plate-plate distance) L=0.1 m, and the air kinematic viscosity ν=1.57×10^{-5} m^2/s).

Fig. 3 shows a typical single image of the flow in the ESP taken by the CCD camera. The dust particles scattering the laser light are visible as bright points in the image.

When no voltage was applied, the submicron dust particles followed the gas main flow and, in this case, the measured velocity field of the particles corresponds to the gas flow velocity field. Fig. 4 shows the particle flow velocity field resulted from averaging of 100 PIV images, which means that the velocity field is time-averaged.

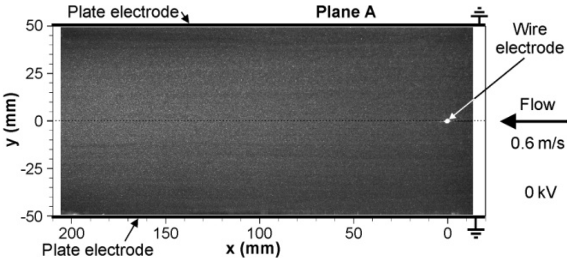

Fig. 3 Instantaneous image of the flow in the ESP when no voltage was applied. Exposure time: 6 ns

The measured flow in the ESP when no voltage was applied was smooth. Small disturbances of the flow were found only in the wake behind the wire electrode. The measured velocity z-component and velocity standard deviation (not presented in this paper) were very low (lower than 0.05 m/s). It means that the flow was practically 2-dimensional and laminar in the observation area when no voltage was applied.

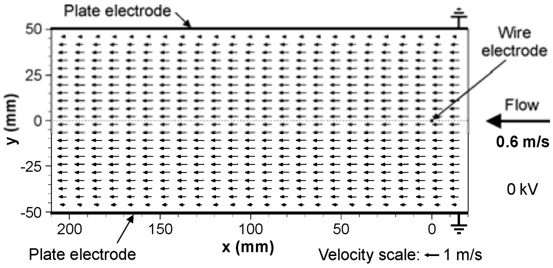

Fig. 4 Averaged flow velocity field in the Plane A in the ESP when no voltage was applied

When a high voltage was applied to the wire electrode, the electric force exerted by the corona discharge and electric field induce a considerable EHD secondary flow of the gas which altered significantly the primary laminar flow.

Figs. 5–14 show the results of the 3D PIV measurements in the ESP when a high voltage was applied. The EHD number, which is related to the electric force, was calculated using a formula: Ehd=$I \times L^3/(\nu^2 \times \rho \times \mu_i \times A)$ [6], where: I - the average total discharge current, L=0.1 m-the distance between the collecting electrodes, ν=1.57×10^{-5} m^2/s - the air kinematic viscosity, ρ=1.205 kg/m^3 - the air density, A = 0.04 m^2 - the discharge area and μ_i=2×10^{-4} m^2/Vs – N_2^+ ion mobility for positive discharge and μ_i=2.7×10^{-4} m^2/Vs – O_2^- ion mobility for negative discharge. The ratio of the EHD number to the Reynolds number squared (describes the ratio of the electric forces to the inertial force) was also calculated.

The instantaneous images of the particle flow in the planes A, B, C and D in the ESP for a positive voltage of 19.5 kV and 28 kV are presented in Figs. 5 and 6, respectively. As it can be seen from Fig. 5a, for a voltage of 19.5 kV (Ehd/Re^2=0.57), in the Plane A the dark trail with brighten borders appeared behind the discharge wire electrode. The dark trail is the area of the ESP in which the dust particles were removed due to the electrical forces (there is no laser light scattered on the dust particles). The brighten borders means the areas with increased dust concentration. This dark trail with brighten borders was very stable and was observed in all images measured at this conditions.

In the Plane B (Fig. 5b) we can observe a different flow structure with two dark trails. The change in the flow structure is probably due to the side wall effect (Plane B was placed 60 mm from the side wall) which disturb the discharge and the flow. For Ehd/Re^2=0.57 the inertial force dominate over the electric force and can easily destabilize very regular flow structure which occurred in the Plane A (midplane of the ESP duct).

Influence of the side wall effect was also observed in Planes C and D (Figs. 5c and 5d) placed 20 mm and 10 mm from the side wall, respectively. In these planes we can observe behind the wire electrode quite irregular Karman vortex like structures.

For the positive voltage of 28 kV, in the Plane A (Fig. 6a), the dark trail behind the wire electrode was observed. However, this structure spreads and was mixed about 70 mm behind the wire electrode (x=70 mm) by the turbulent flow occurred in the ESP during the discharge. At such a high voltage the Ehd/Re^2 ratio equals 3.75 - the electric force dominate over the inertial one. At this conditions also the flow instabilities occurred near the plate electrodes. Irregular vortices arisen before the wire electrode and were floated by the primary flow. In the Plane B (Fig. 6b), the flow structure was very similar to that observed in the Plane A (Fig. 6a). It means that the side wall effect was not strong enough to disturb flow structure ("generated" by the discharge) occurred in the central part of the ESP duct. However, the side wall effect was strong enough to disturb flow structures in Planes C and D (Figs. 6c and 6d). In these planes the wake behind the wire electrode was irregular, turbulent and spreads to the plate electrodes.

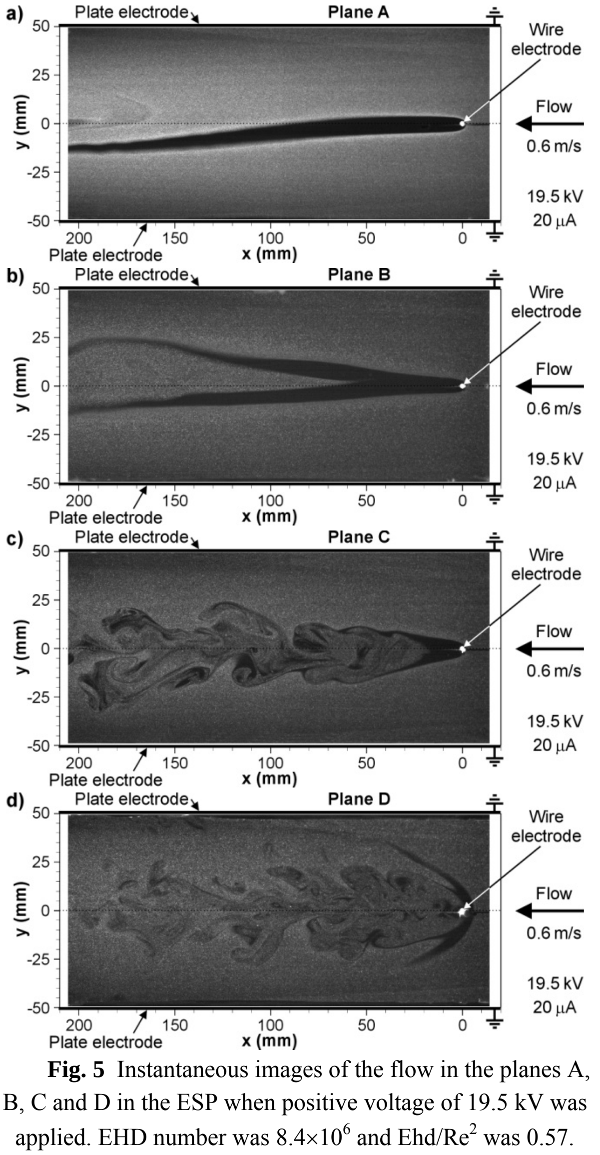

Fig. 5 Instantaneous images of the flow in the planes A, B, C and D in the ESP when positive voltage of 19.5 kV was applied. EHD number was 8.4×10^6 and Ehd/Re^2 was 0.57. Exposure time: 6 ns

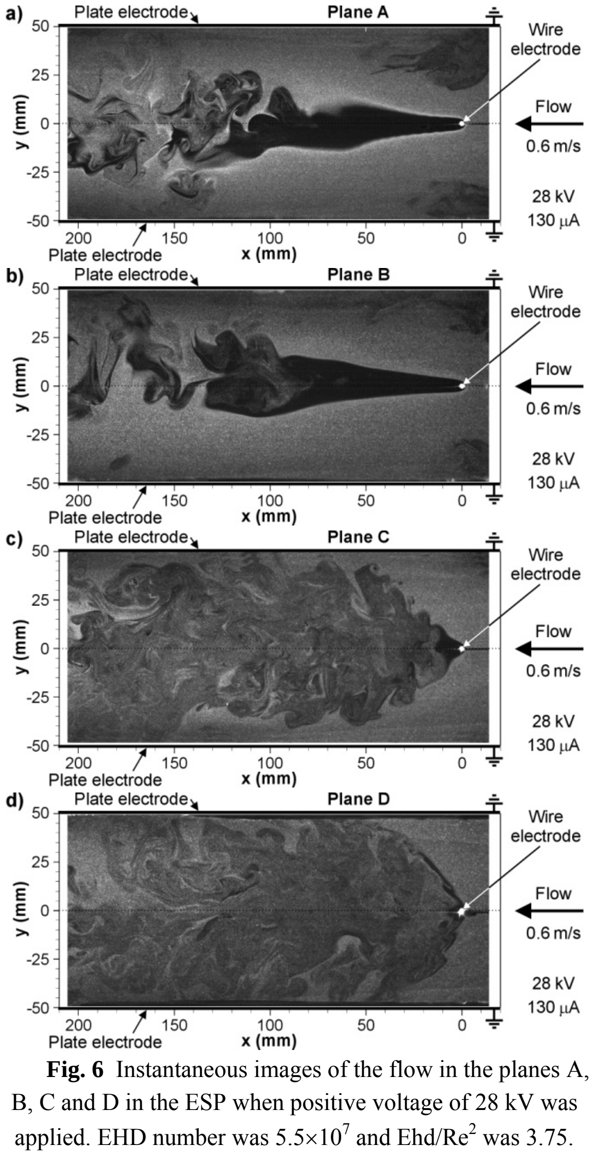

Fig. 6 Instantaneous images of the flow in the planes A, B, C and D in the ESP when positive voltage of 28 kV was applied. EHD number was 5.5×10^7 and Ehd/Re^2 was 3.75. Exposure time: 6 ns

Figs. 7 and 8 show instantaneous images of the particle flow in the planes A, B, C and D for a negative voltage of -19.5 kV and -28 kV. For the voltage of -19.5 kV (Ehd/Re^2 =0.43) in the Plane A (Fig. 7a) the flow structure is much less regular than it was observed for positive voltage (Fig. 5a). The difference between these flow structures certainly originate from the difference between the positive and the negative discharge. For the positive voltage we have uniform discharge along the wire electrode while negative discharge has a form of tufts which occur irregularly.

The instantaneous image obtained for negative voltage of -19.5 kV in the Plane B is presented in Fig. 7b. The flow structure measured in the Plane B was similar to that observed in the Plane A (Fig. 7a) unlike it was for 19.5 kV of positive voltage (the flow structures in Planes A and B were different). It suggest that in the Plane B for the negative voltage the influence of the side wall effect on the discharge is weaker than for the positive voltage. The flow structure for the negative voltage is much more irregular however occur in wider area of the ESP duct (wider in the z-direction i.e. along the wire).

For negative voltage of -19.5 kV in Planes C and D side wall effect is clearly seen. In the Plane C (Fig. 7c) irregular wake spreads behind the wire electrode. In the Plane D (Fig. 7d) there is no wake just behind the wire electrode and vortex structures can be seen about 70 mm behind the wire electrode (x=70 mm) in the centre between the plate electrodes and about 180 mm behind the wire electrode (x=180 mm) near the plate electrodes. Flow structures observed in the Plane D suggest that there was no discharge (no tufts on the wire electrode) in this plane placed 10 mm from the side wall. The vortex structures observed 70 mm and 180 mm behind the wire electrode certainly flow from aside crossing the Plane D.

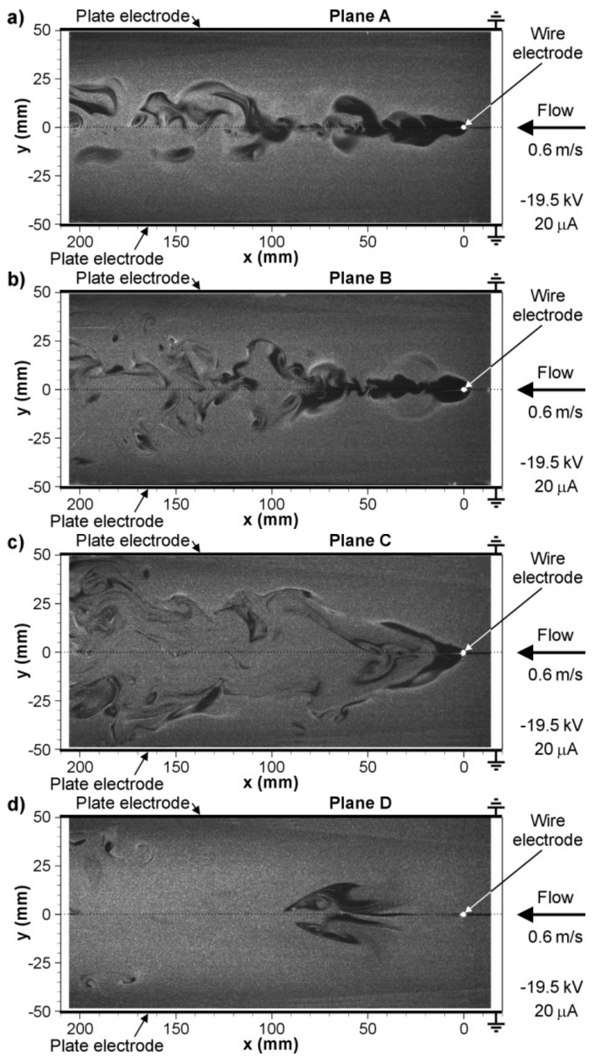

Fig. 7 Instantaneous images of the flow in the planes A, B, C and D in the *ESP* when negative voltage of -19.5 kV was applied. EHD number was 6.2×10^6 and Ehd/Re^2 ratio was 0.43. Exposure time: 6 ns

The instantaneous images of the particle flow in the planes A, B, C and D in the ESP for a negative voltage of -28 kV (Ehd/Re^2=3.2) are presented in Fig. 8. As it can be seen, the flow structures in the Planes A and B (Figs. 8a and 8b) are very similar. The irregular wake, Karman vortex like structure, started arising behind the wire electrode, but it was immediately scattered by irregular flow disturbances. Similarly like for positive voltage of 28 kV, the irregular vortices arisen near the plate electrodes and were floated by the primary flow. The flow structures in the Planes C and D (Figs. 8c and 8d) were irregular, turbulent and spread to the plate electrodes. In the Plane D there were flow disturbances near the wire electrode. It suggest that for negative voltage of -28 kV there were tufts on the wire electrode (unlike for the negative voltage of -19.5 kV).

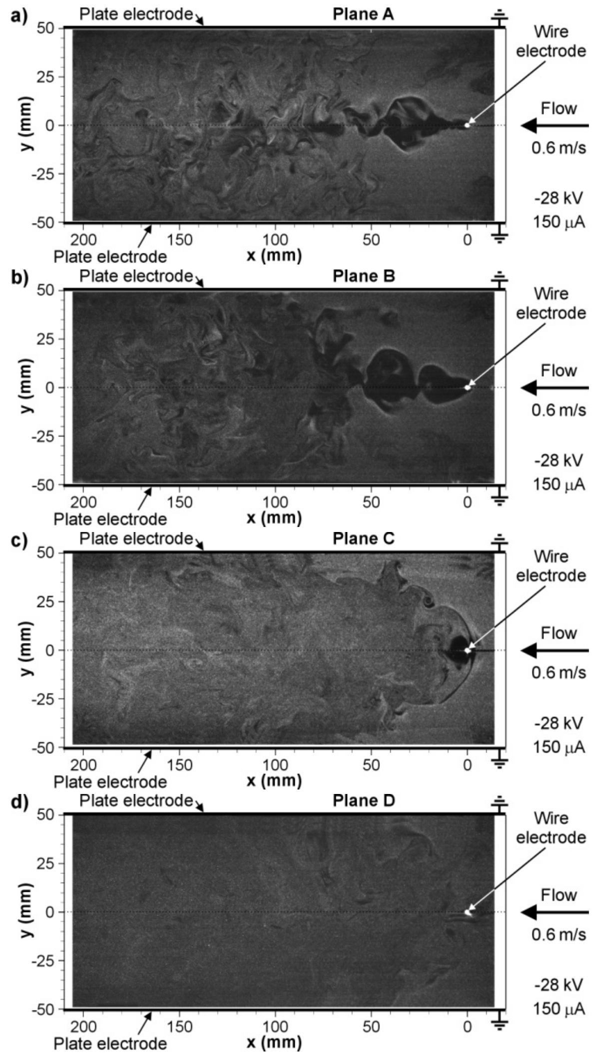

Fig. 8 Instantaneous images of the flow in the planes A, B, C and D in the ESP when negative voltage of -28 kV was applied. EHD number was 4.7×10^7 and Ehd/Re^2 was 3.2. Exposure time: 6 ns

Averaged flow velocity fields measured by 3D PIV are presented in Figs. 9-12 as vector maps and colour (greyscale) maps. Vectors show velocity *x*- and *y*-component. Colour maps show velocity *z*-component (perpendicular to the measurement plane).

Averaged flow velocity fields in the Plane A for positive and negative discharge are presented in Figs. 9 and 10, respectively. Although instantaneous flow structures for positive and negative discharge are different, averaged low velocity fields are similar. For both polarities, in the discharge region vortices blocked the flow near the plate electrodes and gas flowed by the central part of the ESP duct, close to the wire electrode. After passing the wire electrode the flow spreads up to the plate electrodes. In the downstream of the discharge region (*x* from 50 mm to 205 mm) flow patterns became quite regular. The flow velocity *z*-component (Figs. 9b and 10b) in almost whole observation area was very low (lower than 0.05 m/s) and only near the plate electrodes and for positive polarity in the wake behind the wire electrode it reaches values up to 0.15 m/s.

Low average velocities in the *z*-direction measured in the Plane A (midplane) in the wide ESP means that the time-averaged EHD secondary flow was practically 2-dimensional. However, the analysis of instantaneous velocity fields (not showed in this paper) exhibit that the EHD flow is turbulent with a relatively high instantaneous velocity *z*-component (up to 0.45 m/s). It means that even in wide ESPs the EHD flow cannot be assumed to be 2-dimensional when its short-time flow behaviour is considered. Detailed analysis of instantaneous and time-averaged flow patterns in the midplane of the wide ESP is presented in [7].

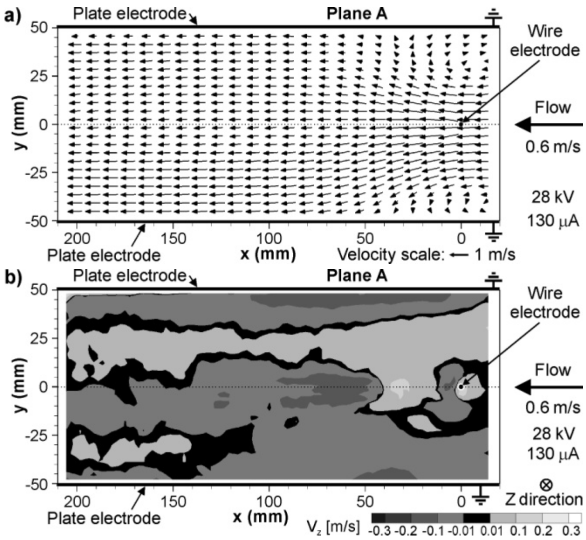

Fig. 9 Averaged flow velocity field in the Plane A in the ESP. Positive voltage of 28 kV was applied. EHD number was 5.5×10^7 and Ehd/Re^2 was 3.75

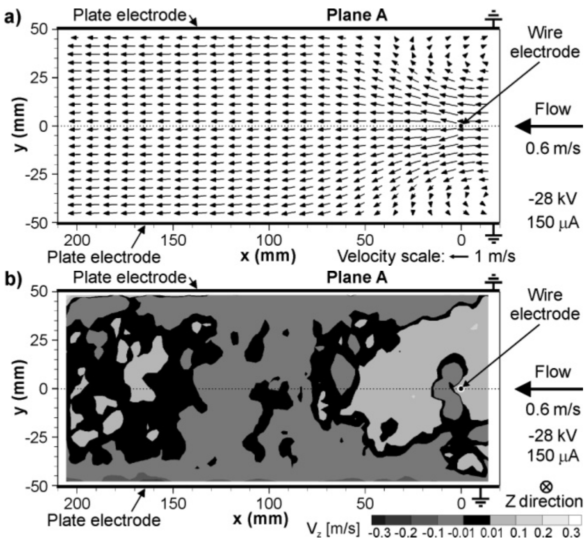

Fig. 10 Averaged flow velocity field in the Plane A in the ESP. Negative voltage of -28 kV was applied. EHD number was 4.7×10^7 and Ehd/Re^2 was 3.2

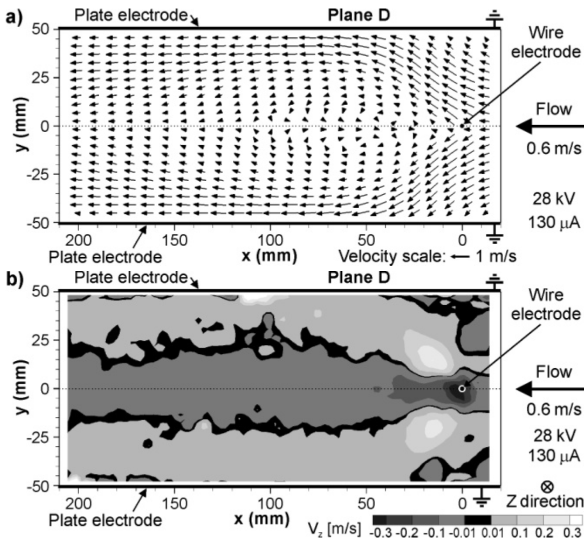

Fig. 11 Averaged flow velocity field in the Plane D in the ESP. Positive voltage of 28 kV was applied. EHD number was 5.5×10^7 and Ehd/Re^2 was 3.75.

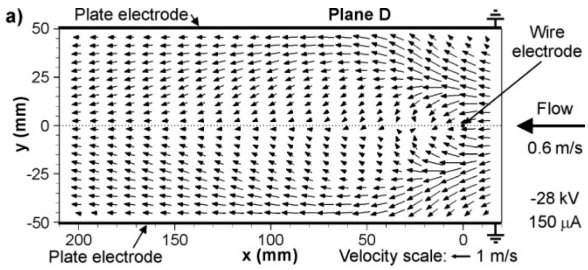

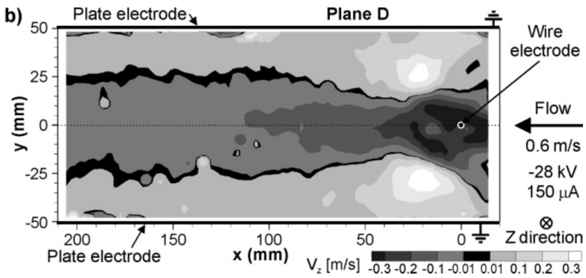

Fig. 12 Averaged flow velocity field in the Plane A in the ESP. Negative voltage of -28 kV was applied. EHD number was 4.7×10^7 and Ehd/Re^2 was 3.2

Averaged flow velocity fields in the Plane D (placed 10 mm from the side wall) for positive and negative discharge are presented in Figs. 11 and 12, respectively. As it can be seen from vector maps (Figs. 11a and 12a), in the downstream of the wire electrode the flow was blocked in the centre of the ESP duct and the gas flows near the plate electrodes. The averaged velocity *z*-component (Figs. 11b and 12b) for both voltage polarities has similar structure. Near the plate electrodes the gas flows to the side wall while in the central part of the ESP duct the gas flows in the opposite direction. The averaged velocity *z*-component in the Plane D reaches the values up to 0.3 m/s for positive voltage polarity and up to 0.45 m/s for negative voltage polarity. High values of averaged velocity z-component suggest that in the vicinity of the Plane D the discharge strongly change along the wire electrode (along the *z*-direction).

4 CONCLUSIONS

In this paper, the 3D PIV velocity field measurements in four parallel planes set along the ESP duct are presented. The first plane was placed in the ESP midplane when the other planes were placed 60 mm, 20 mm and 10 mm from the side wall.

Obtained results showed that the time-averaged flow in the midplane of the wide ESP is almost 2-dimensional. However, the measured flow was turbulent with a relatively high instantaneous velocity z-component. Therefore, the flow in the midplane of the wide ESP cannot be assumed to be 2-dimensional when its short-time behavior is considered.

The analysis of results obtained in all four measurement planes showed strong influence of the side wall on the discharge and, in consequence, on the flow patterns occurred in the ESP. However, this influence seems to be different for particular voltage polarity. One can deduce that tufts characteristic for the negative discharge have quite similar strength along the discharge wire electrode and immediately fade close to the side wall. For the negative voltage of -19.5 kV tufts faded between Plane C placed 20 mm from the side wall and Plane D placed 10 mm from the side wall (there was no discharge in the Plane D). For the positive voltage polarity the discharge is weaker and weaker towards the side wall. Nevertheless, for the positive voltage of 19.5 kV there was a discharge in the Plane D i.e. closer to the side wall than it was for the negative voltage. Higher value of the average velocity z-component measured in the Plane D for the negative voltage seems to confirm supposition that near the side wall there was much more drastic change in discharge behavior and consequently in flow than observed for the positive polarity.

Moreover, one can notice that the side wall effect is stronger for the lower voltage. For the positive voltage of 19.5 kV the side wall effect was clearly seen in the Plane B (placed 60 mm from the side wall) while for the positive voltage of 28 kV the side wall effect was seen in the Plane C (placed 20 mm from the side wall). For the positive voltage of 28 kV the flow pattern in the Plane B was very similar to that observed in the midplane of the ESP (i.e. side wall effect was not observed).

ACKNOWLEDGEMENTS

This research has been supported by the State Committee for Research and Development (grant PB 1857/B/T02/2007/33).

REFERENCES

1. Mizuno. Electrostatic precipitation, IEEE Trans. Diel. Electr. Insul. 2000, 7: 615-624.
2. P. Atten, F. M. J. McCluskey, A. C. Lahjomri, The Electrohydrodynamic origin of turbulence in electrostatic precipitators, IEEE Trans. Ind. Appl. 1987, 23: 705-711.
3. P. Atten, H. L. Pang, J. L. Reboud, J. Podliński, J. Mizeraczyk. Turbulence generation by charged fine particles in electrostatic precipitators, in Proc. ESA Annu. Meeting on Electrostatics 2007, Laplacian Press 2007, 259-270.
4. U. Kogelschatz, W. Egli, E.A. Gerteisen, Advanced computational tools for electrostatic precipitators, ABB Review 1999,4: 33-42.
5. M. Raffel, Ch. E. Willert, J. Kompenhans, Particle Image Velocimetry, A practical guide, Springer-Verlag Berlin Heidelberg, 2007.
6. IEEE-DEIS-EHD Technical Committee, Recommended international standard for dimensionless parameters used in electrohydrodynamics, IEEE Trans. Diel. Electr. Insul. 2003, 10-1: 3-6.
7. J. Podliński, P. Atten, J. Mizeraczyk, Instantaneous and time-averaged velocity fields in a wide electrostatic precipitator, in 6th Conference of the French Electrostatics Society, SFE'2008, Gif-sur-Yvette 2008, 142-149.